AEROSTAT EFFECT ON UAV STABILITY

By

Ahmed Yosreldin Eisa Musa

20476

Dissertation submitted in partial fulfilment of

The requirements for the

Bachelor of Engineering (Hons.)

(Mechanical)

March 2016

Universiti Teknologi PETRONAS

Bandar Seri Iskandar

31750 Tronoh

Perak Darul Ridzuan

CERTIFICATION OF APPROVAL

AEROSTAT EFFECT ON UAV STABILITY

By

Ahmed Yosreldin Eisa Musa Fadlelmoula
20476

A project dissertation submitted to the
Mechanical Engineering Programme
Universiti Teknologi PETRONAS
in partial fulfilment of the requirement for the
BACHELOR OF ENGINEERING (Hons)
(MECHANICAL)

Approved by,

_____

(Name of Main Supervisor)

UNIVERSITI TEKNOLOGI PETRONAS
TRONOH, PERAK
8 April 2016

CERTIFICATION OF ORIGINALITY

This is to certify that I am responsible for the work submitted in this project, that the original work is my own except as specified in the references and acknowledgements, and that the original work contained herein have not been undertaken or done by unspecified sources or persons.

_____

AHMED YOSRELDIN EISA MUSA

ABSTRACT

The current generation of UAVs lack extended hovering and flight capabilities. Equipping a quadrotor with an inflatable structure enhances energy efficiency. In this work, the aerostat size effect on a UAV quadrotor system is investigated, and the stability of the Lighter-than-Air system is contrasted by creating a flight dynamics model. A mathematical model of the AR DRONE 2.0 with an aerostat is formulated and simulated with Matlab in hovering mode. The mathematical model is validated by comparison to real-life flight data. A validated dynamic model describing the behavior of the drone in hovering mode was developed and used for simulation.

ACKNOLWEDGEMENTS

Table of Contents

LIST OF FIGURES

LIST OF TABLES

CHAPTER 1

INTRODUCTION

1.1 BACKGROUND

Unmanned Air Vehicles (UAVs) are autonomous aircrafts that operate without a pilot, and are guided remotely. UAVs have many applications in both civil and military domains, to carry out different roles and missions. They have become a significant research topic in the last decade; and several enhancements could be introduced in certain areas in order to further expand their applications.

The vast majority of UAVs are powered by batteries and the aircraft have to be landed and recharged at some point. Thus, power consumption is the main determinant of flight duration.

Aerostats supporting the weight of the aircraft could enhance the UAV capabilities. QinetiQ's team adapted the technology in their solar powered UAV, the Zephyr 4 [1] [2]. The team used the concept to design an inflatable launching structure of a helium balloon, to ensure their UAV gains sufficient attitude and stay aloft for an extended period of time. The Zephyr 4 underwent a test flight, where it flew for one hour after being launched at 30,000ft by the balloon.

Moreover, Edge et al. [3] explored, developed and demonstrated the concept of Pressurized Structure-Based (PSB) technology. Their work investigated envelope design and fabric materials of the structure by evaluating and simulating several models in X-Plane flight simulator.

For many years, aircraft designers have used tried-and-true rules of thumb and iterations on previous stable designs to help ensure the stability of their new designs. However, improved knowledge of dynamic systems and fluid analysis allows modern

designers to predict an aircraft's qualities with approximate mathematical models, and simulation software [4].

1.2 PROBLEM STATEMENT

Investigating the effect of upgrades and improvements on UAVs is a tedious process that risks damages to the system. Aircrafts employing buoyancy are inherently unstable in flight mode. By creating a mathematical model of the aerostat-UAV, the dynamic behavior of the system can be predicted and it can be tested, designed, and implemented.

1.3 OBJECTIVES

- To study the aerostat size effect on UAVs.
- To contrast the stability of a UAV equipped with an aerostat.

1.4 SCOPE OF STUDY

The study is limited to the Parrot AR DRONE 2.0, a small UAV Quadcopter. It aims to investigate the stability and aerostat effects on the system, by experimenting with a validated mathematical model. The model describes the hovering behavior of the drone.

CHAPTER 2

LITERATURE REVIEW

2.1 DYNAMIC MODEL BUILD UP

Luukkonen [5] presented a simple mathematical model of the quadcopter dynamics, wherein aerodynamic effects were neglected and the quadrotor motors were not modelled; since it would require estimations of the motor parameters, unlike Meyer et al.'s model [6] which contrasted that the system dynamics are directly related to the thrust and torque induced by each propeller unit. The parameters of the model, such as masses, moments of inertia, and aerodynamics, were obtained by wind tunnel simulations. The model was constructed using an open source simulator Gazebo, and the results were validated against real flight data. Additionally, Tayebi & McGilvray [7] modeled the system with an additional gyroscopic term, caused by the rotations of the airframe and the four rotors. The dynamic model proposed by Hamel et al. [8] of an X4-flyer included the airframe, motor dynamics, and rotor aerodynamics and gyroscopic effects.

The dynamic model is then tested and compared to the actual model behavior, in order to validate the results, by testing flight trajectories as shown in Figure 1 [6]. Euler angles and altitude signals can be compared as a validation method as well.

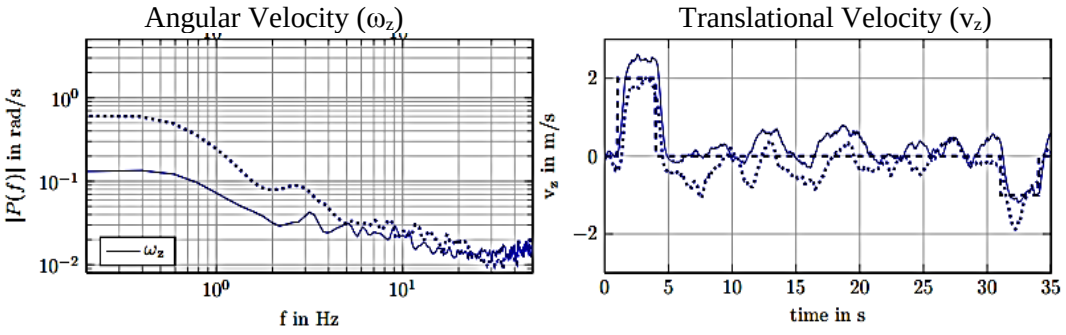

FIGURE 1. Comparison of simulated and measured velocities. Dotted lines represent measurements while solid lines are simulated data. (Source: [6])

However, validation results may be obtained through simulation only, but might prove unrealistic [5], [9], [10].

Most approaches of quadrotor modelling are carried using software such as Matlab [5], [8], [11], [12], Robotic Operating System (ROS) and Gazebo [6], and Microsoft Excel [13].

2.2 DYNAMIC MODEL STABILIZATION

Aircrafts possess dynamic stability if the amplitudes of a motion induced by a disturbance eventually decrease to zero relative to a steady-state flight condition [14].

Pounds et al.'s work [15] investigated the stability bounds of a quadcopter; within which an added force to the system will not change or destabilize the aircraft. It was concluded that the stability behavior of quadrotors is related to helicopters. This simplification of the dynamic model could provide substantial data and results for research regarding quadrotors, however key differences are noted such as the tip-path plane which is described by helicopter blades during their rotation. For helicopters, the rotor disc is permitted to tilt under certain conditions such as maneuvering, therefore the thrust is not always perpendicular to the rotor shaft. Another difference is blade flapping - up and down movement of the blade due to airspeed- which causes dissymmetry in the lift and results in system vibrations.

In [7], the dynamic stability is analyzed by the differential equations of aircraft motion. Newton Law's, quaternions and matrices are used to simply describe the UAV's Euler angles, providing easier and acceptable results.

Samuelsson [16] refers to static stability as the pitching moment variation with angle of attack for different flight scenarios. However, coefficients for the moments about the body axes of the UAV require separate study with complex calculations and exact design parameters.

In summary, there are several approaches to model the dynamic behavior of quadrotors, [15] approximated the stability of a helicopter, and [5] excluded the effects of aerodynamics and the motors, unlike [6] which only modeled thrust and

torque induced by the motors. In [7] and [8] gyroscopic terms were added along with aerodynamic effects, motor, and rotor dynamics to describe the flight dynamics.

Authors	Review	Analysis
[15]	Quadrotors dynamic behavior are similar to helicopters.	Quadrotor thrust is always perpendicular to Rotor Shaft. Quadcopters blade flapping can be negligible
Luukkonen, Teppo (2011).	Modelling basic Structures of Quadcopter dynamics Aerodynamic Effects excluded Motors were not modeled	Incomplete modelling of the system dynamics Unreliable behavior and not validated
Meyer, J.; Sendobry, A.; Kohlbrecher, S.; Klingauf, U.; von Stryk, O. (2012).	Motors' thrust and torque determine overall dynamics Validation of simulation results	Parameters obtained are both accurate and valid. Complex Wind tunnel parameterization
Tayebi, A.; McGilvray, S. (2004).	Addition Gyroscopic term due to the rotation of Airframe and rotors	Further enhances the model accuracy, and stability.
Hamel, Tarek; Robert, Mahony; Lozano , Rogelio; Ostrowski, James (2002).	Dynamic model included airframe, motor dynamics, and both aerodynamic and gyroscopic effects of the rotors.	Gives complete and accurate results Complex parameterization of the system.

CHAPTER 3

RESEARCH METHODOLOGY

3.1 PROJECT OUTLINE

This project's focus is the "Parrot AR DRONE 2.0", a small commercial quadcopter with Wi-Fi control, and specifications as shown in Appendix A and B. by measurements and experimentation, the required physical parameters are determined. The parameters are used to form a graphical mathematical model using Simulink in Matlab environment. Initial simulation results are collected and validated against the actual UAV system dynamics, by comparing altitude, pitch, and roll signals. Finally, the mathematical model is used to accomplish the objectives of the project; to investigate the aerostat size effect and to contrast the stabilities of UAV systems with and without an aerostat, by forming and linking a representative subsystem to the model.

3.2 PROJECT ACTIVITIES

The final outcome of the project is a controllable dynamic model describing the dynamic behavior of the AR Drone 2.0, with an inflatable structure, i.e., aerostat. The project activities are as follows:

1) Introduction to the AR DRONE 2.0 and controls via ROS: using the Robotic Operating System (ROS) drivers to control the drone via keyboard and communicate with various sensors in order to record flight data.

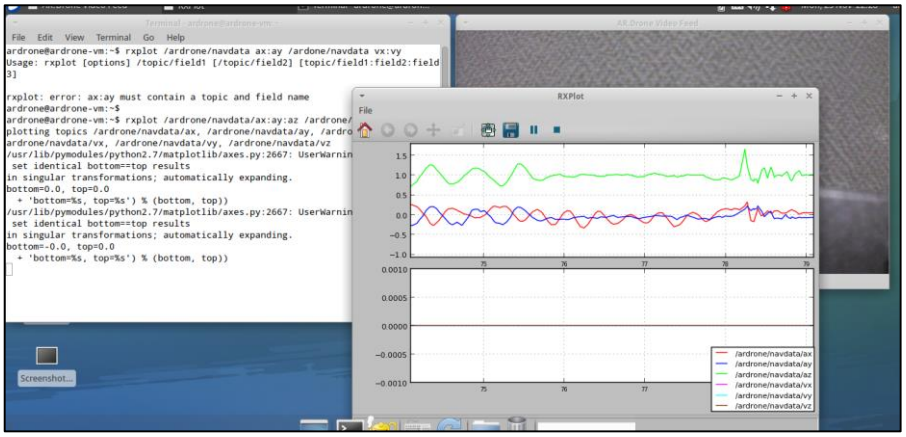

FIGURE 2. Robotic Operation System capturing sensors' data.

2) Estimation of parameter values to be used in the simulation:

the geometrical data and physical constants such as masses and moments of inertia. Direct measurements and manufacturer's specifications are used to obtain the parameters. Basic assumptions are shown in Table 1 below.

TABLE 1. Parameters' estimation assumptions.

Assumptions
1. The structure of AR Drone is rigid and highly symmetrical.
2. The propellers are rigid and the thrust is parallel to the axis of the rotors.
3. The center of gravity of AR Drone and the origin of the body frame coincide.
4. No turbulence and airflow through the rotor indoors.
5. The model neglects blade flapping.

3) Mathematical model of the AR Drone 2.0 using Matlab's Simulink:

The software uses solvers to compute the dynamic system states at successive time steps over a specified time span, by using the model parameters. By applying numerical methods, the set of ordinary differential equations that represent the model are solved. The model is constructed using block functions in Simulink, along with a graphical CAD to represent the UAV's orientation and velocity.

4) Validation of the dynamic model:

by comparing the dynamics of the model against the actual system dynamics in hovering mode, and ensure similar behavior.

5) Addition of the Inflatable structure dynamic model:

By modifying the mathematical model to include buoyancy forces, which depends upon the lifting gas. Helium is usually the lifting gas of choice, because it is chemically

inert and has the second lowest density of any gas [17]. The inflatable structure is designed to fit on the AR DRONE indoor hull.

6) Simulation and analysis of the simulation results:

by comparing to the original model in terms of dynamic stability and power consumption by motors for a specific flight trajectory.

The project flowchart is illustrated in Figure 3.

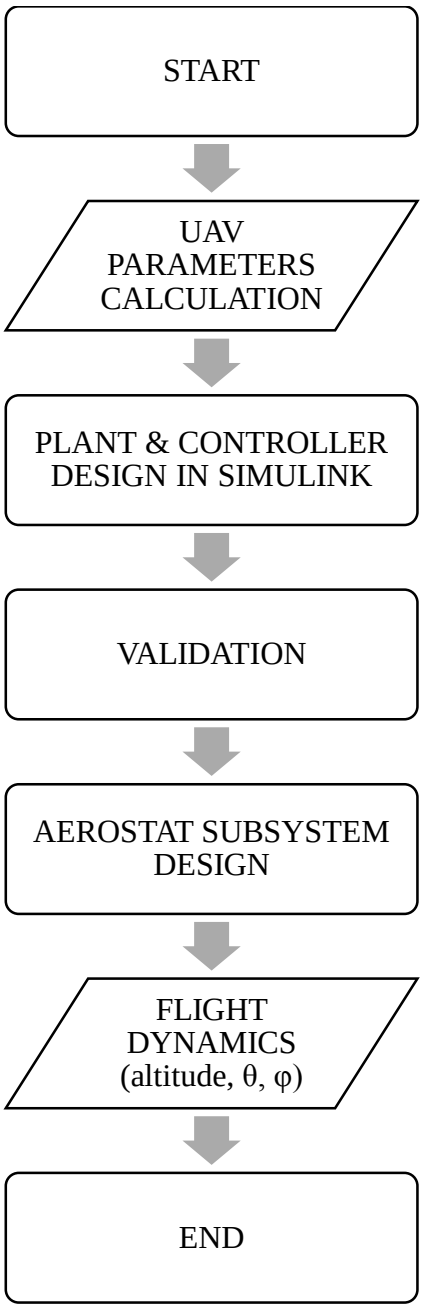

FIGURE 3. Workflow of the Project

3.3 KEY MILESTONES

- Completion of the dynamic model of the AR DRONE 2.0.
- Validation of simulation results.
- Completion of the dynamic model of the Inflatable Structure.
- Completion of simulation and analysis of the Inflatable LTA system.

3.4 GANTT CHART

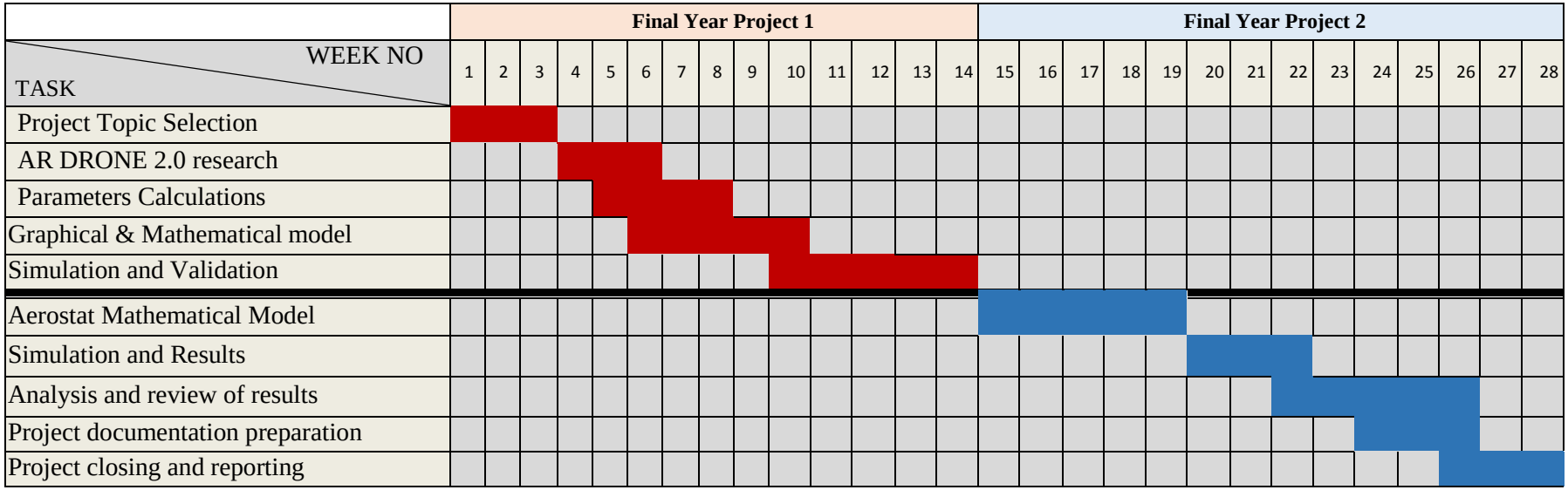

3.5 SOFTWARE/HARDWARE REQUIRED.

- AR DRONE 2.0.
- Matlab 2015b Simulink Toolbox.
- ROS Groovy.

3.6 PROJECT METHODOLOGY

3.6.1. CAD model design

In order to simulate the physical system of the AR DRONE 2.0, a CAD model was assembled to estimate the masses and inertial properties as simulation parameters. The CAD model is shown in Figure 4.

FIGURE 4. The AR DRONE 2.0 CAD Model

The total estimated mass is equal to 450 grams and the system parameters can be found in table 2. The parameters are identified via direct measurements and with the aid of SolidWorks for inertial calculations.

TABLE 2. AR DRONE 2.0 simulation parameters

Parameter	Value	Unit	Remarks
g	9.81	m/s^2	Standard gravity
m	0.45	kg	AR DRONE 2.0 mass
I_x	0.002234329	$kg.m^2$	x-axis moment of inertia
I_y	0.002990543	$kg.m^2$	y-axis moment of inertia
I_z	0.004804391	$kg.m^2$	z-axis moment of inertia

3.6.2. Matlab Simulink model

A model was built in Matlab 2015b using the SimMechanics toolbox in Simulink to simulate the system dynamics and responses. The system comprises of a plant and a controller as shown in Figure 5.

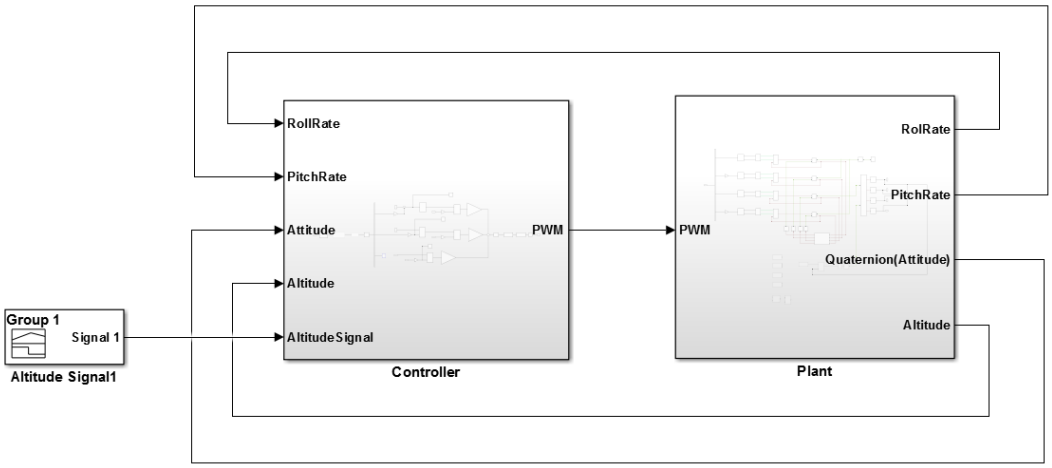

FIGURE 5. Plant and Controller systems.

The model is a closed-loop control system, which utilizes feedback (Roll, Pitch, and altitude signals) from the Plant subsystem to control the motion of the model. A desired altitude signal can be provided to the controller through the "AltitudeSignal" port, and the controller will produce a corresponding signal. The four rotors of the drone are used auxiliary to control the Euler angles.

The Plant contains three main subsystems: Engine dynamics, Rotor dynamics, and Body dynamics, as illustrated in Figure 6.

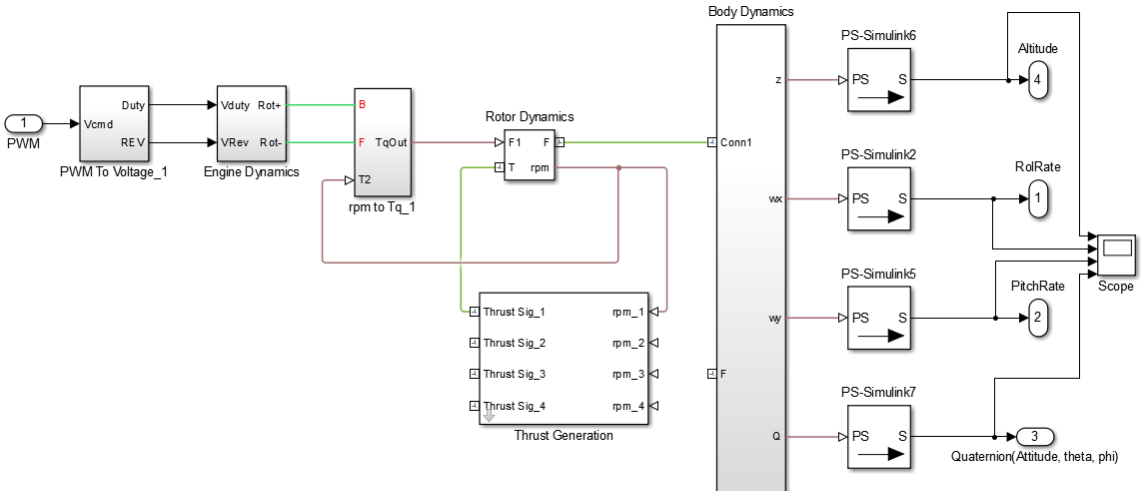

FIGURE 6. The plant's subsystems (simplified)

The Plant is controlled by the input PWM signal from the Controller. The engine dynamic subsystem contains a DC motor block that converts the PWM voltage (v) into an angular velocity (ω). The engine dynamics subsystem is shown in Figure 7.

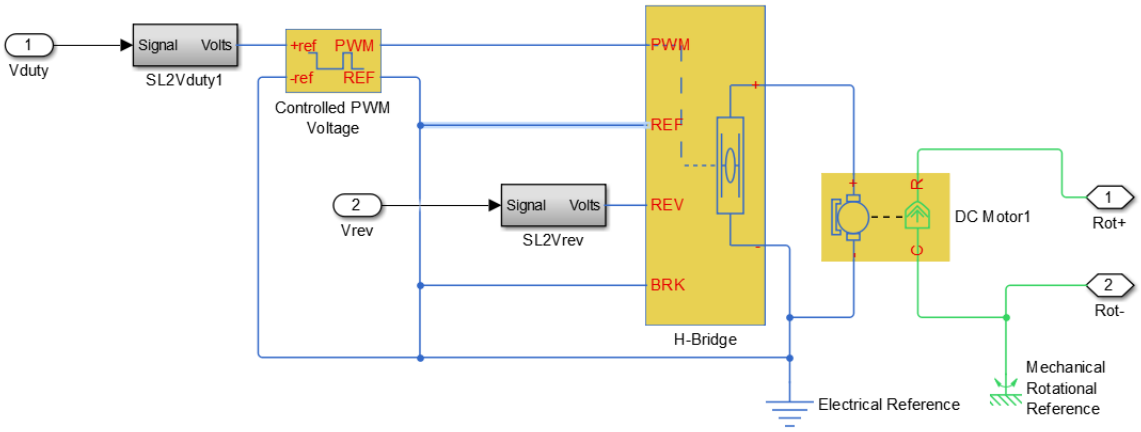

FIGURE 7. Engine dynamics subsystem.

The subsystem output two mechanical Rotational signals (Rot+ & Rot-) that provide rotational motion to the rotor dynamics subsystem. Figure 8. Illustrates the Rotor dynamics subsystem.

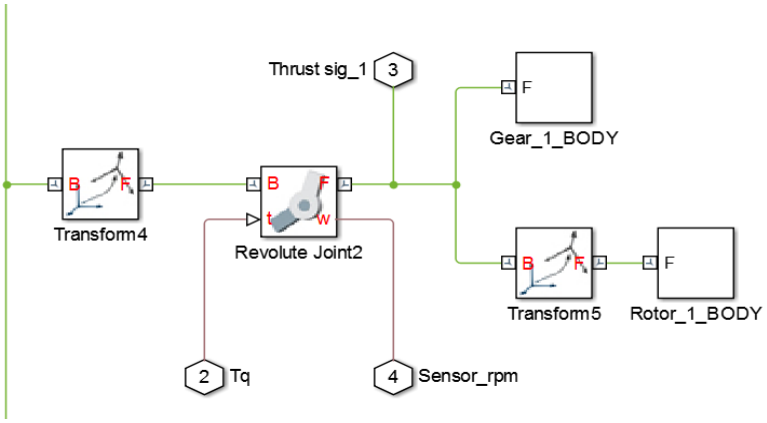

FIGURE 8. Rotor Dynamics Subsystem.

The main component of the rotor subsystem is the revolute joint. The DC motor's Torque (Tq) actuates the joint rotation. The joint rotational rate (Sensor_rpm) is used as a closed loop feedback signal to generate thrust forces. Figure 9 shows the components of the "rpm to thrust" subsystem.

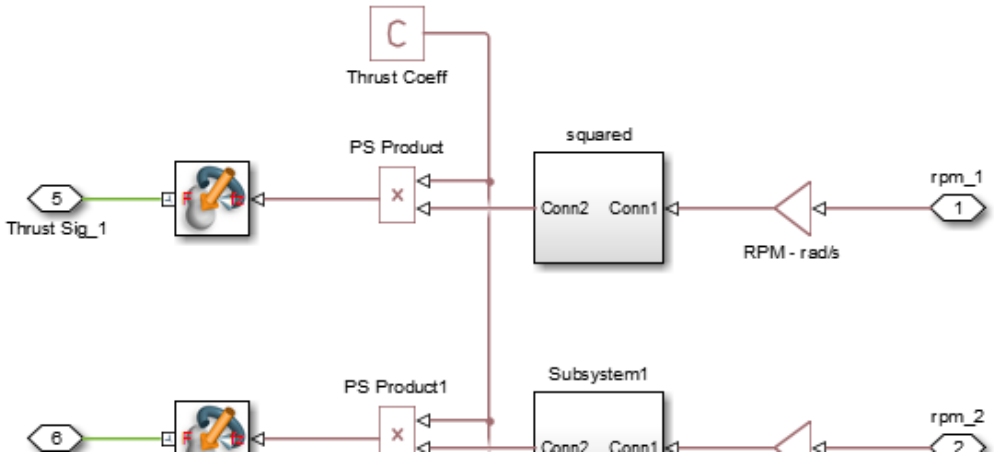

FIGURE 9. Thrust generation subsystem (for one rotor).

The subsystem above used to generate thrust forces. The thrust (T) is proportional to the square of rotational speed:

$$T = C_T.\omega^2 \tag{1.}$$

where C_T is the thrust coefficient, ω is the angular velocity. The value of C_T depends on the geometry of the propellers and the flow conditions. The value of C_T in the model is equal to $C_T = 6.1e-07$ which give the rotational rate of the actual model in RPM.

The body dynamics subsystem accounts for the aerodynamic effects on the aircraft. For simplification, drag force is composed only of the fuselage drag. The fuselage drag term depends on the drag coefficient, size of the body, and the square of velocity:

$$F_D = -\frac{1}{2} C_{dF} \rho A_F v^2 \tag{2.}$$

where C_{dF} is the fuselage drag coefficient and A_F is the cross-sectional area. Figure 10 shows the components of the body dynamics subsystem (refer to detailed Figure C.1 in Appendix C).

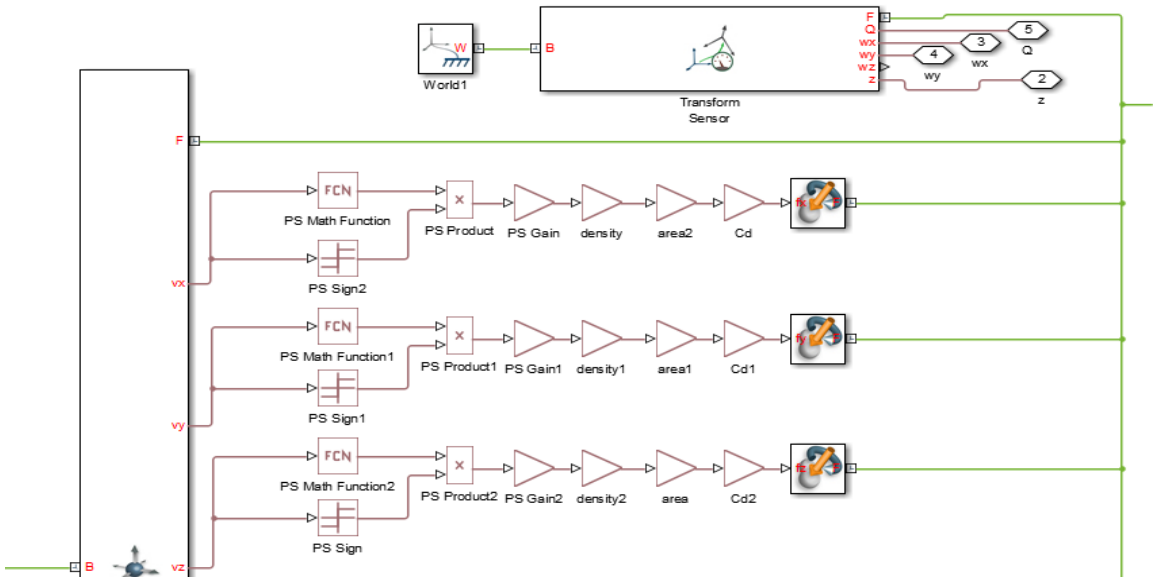

FIGURE 10. Body dynamics subsystem.

The body dynamics subsystem calculates drag forces by measuring velocities in the three directions x, y, and z. The generated forces are linked to the model's body blocks. Pitch (θ), Roll (φ), and Altitude signals of the model are measured by using "Transform Sensors" as shown in Figure 10 above.

3.6.3. Controller design & tuning

The Controller subsystem uses the Euler angles (θ, φ) and altitude feedback to achieve the desired output. The PI and PID controllers generate an error signal from the difference between the feedback and the desired Euler angles. The error signal of each angle is then converted into a PWM command. For example, Figure 11 shows the Pitch angle controller of the model, which is similar to the Roll controller.

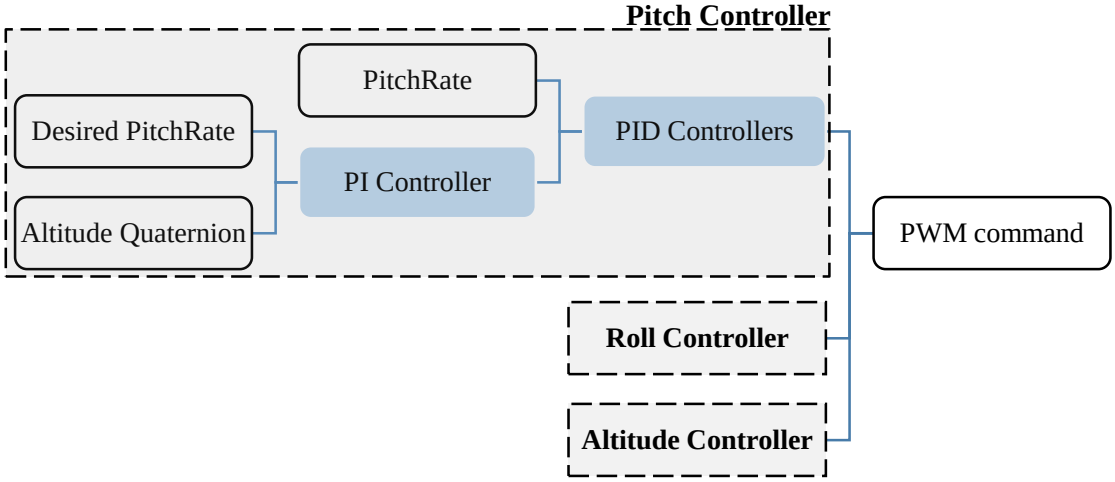

FIGURE 11. Pitch controller.

However, the altitude controller uses a single PID controller with the desired altitude as input in addition to the feedback altitude signal. The error signals are summed to produce a corresponding PWM signal, as shown in Figure 12.

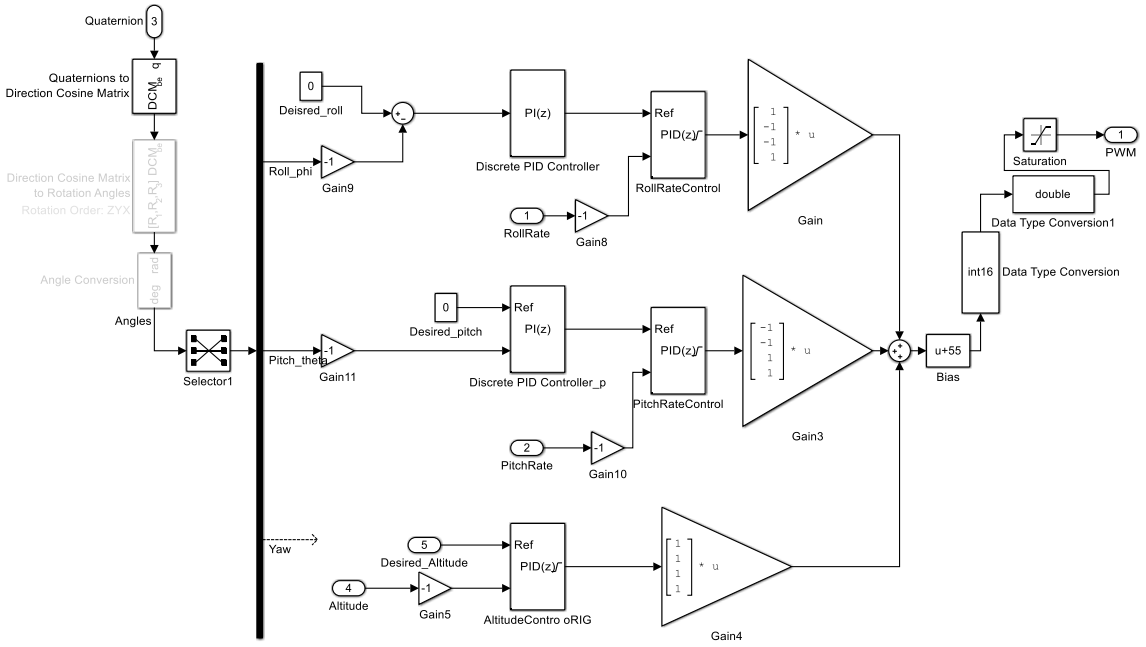

FIGURE 12. Controller Subsystem.

After validating the Simulink model results against the real flight data from of the AR DRONE 2.0, the aerostat subsystem is added to the plant subsystem. An actuating force that resembles buoyancy is exerted at the center of buoyancy of the structure.

3.6.4. Aerostat model

The CAD model of the aerostat and physical parameters are shown in Figure 8 and Table 3 respectively.

FIGURE 13. The AR DRONE 2.0 with an aerostat.

TABLE 3. Aerostat Parameters.

Parameter	Value	Unit	Remarks
M	206.8	kg	Aerostat mass
V	2.25	m^3	Aerostat volume
I_x	0.0016	$kg.m^2$	x-axis moment of inertia
I_y	0.0008	$kg.m^2$	y-axis moment of inertia
I_z	0.0017	$kg.m^2$	z-axis moment of inertia

LTA flight is possible due to buoyancy. The buoyant force must be greater or equal to the weight of the object, in order to achieve positive buoyancy [18]. The buoyant force of an object is calculated by:

$$L_b = (\rho_{air} - \rho_{obj}).V.g \tag{3.}$$

where ρ is density, V is volume, and g is standard gravity.

The aerostat dynamics subsystem and the resulting buoyancy force are added to the model and linked to the center of gravity of the "Body dynamics" subsystem. Three sizes of aerostat envelope (1.5 m^3, 1.0 m^3, and 0.75 m^3) are experimented with and used to calculate the buoyancy forces and test the effects on the virtual model. The lifting gas used is Helium ($\rho_{helium} = 0.164\ kg/m^3$).

The aerostat subsystem components are shown in Figure 14 below.

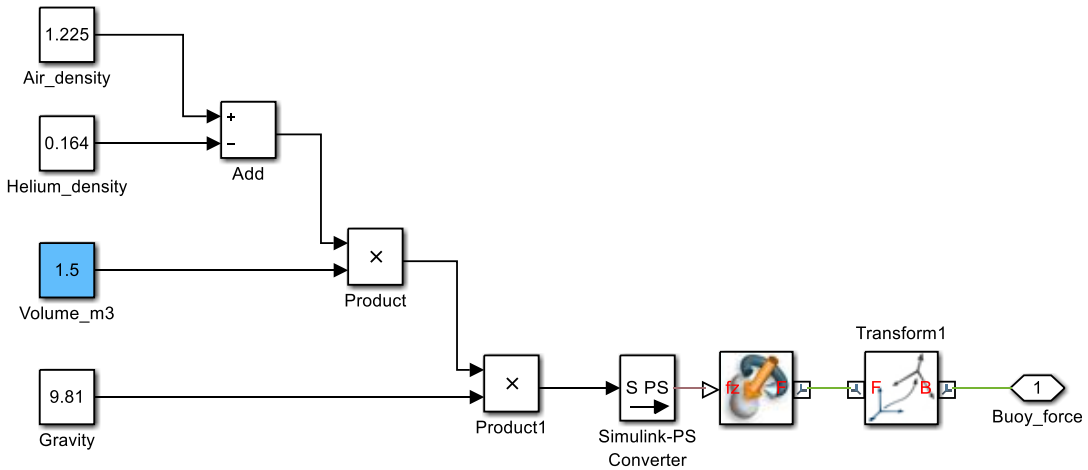

FIGURE 14. The aerostat subsystem

CHAPTER 4

RESULTS AND DISCUSSION

4.1 Simulink Model Validation

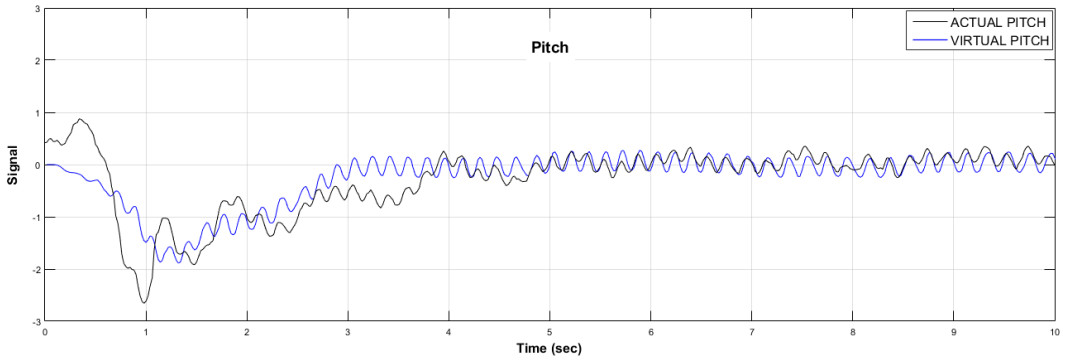

FIGURE 15. Actual and virtual pitch signals.

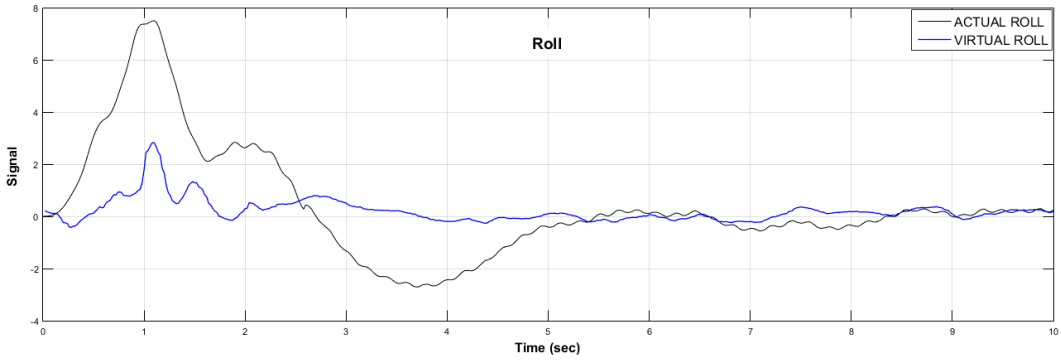

FIGURE 16. Actual and virtual roll signals.

Figures 15 and 16 above show the actual pitch and roll signals acquired from the AR DRONE 2.0 on-board sensors in comparison to the Simulink virtual model's signal. There is a discrepancy in the transient part of the signal, caused by the difference in controllers' parameters and the difficulty to replicate the actual PID parameters.

Additionally, the AR DRONE 2.0 utilizes an on-board camera to analyze patterns in order to control and stabilize the system. Using patterns as a stabilization method

causes the AR DRONE 2.0 to experience random movements the virtual model cannot replicate.

Moreover, it is difficult to obtain precise model parameters such as masses, moments of inertia, and motor coefficients that are identical to the actual system. Limitations of the dynamic model, such as simplified assumptions and negligence of environment factors (such as wind, turbulence, and airflow through the rotor) also lead to discrepancies. However, it is noted that the signals converge in the steady-state region and the errors decrease.

4.2 Aerostat size effect

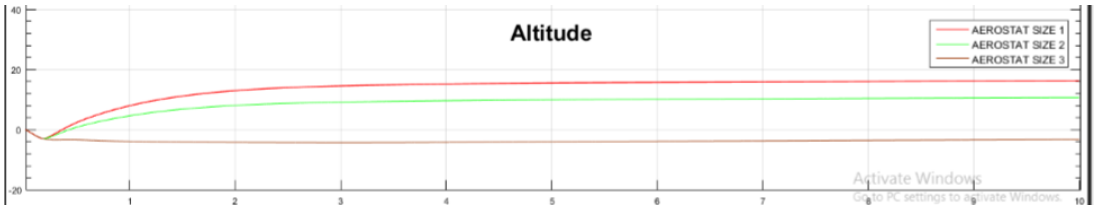

FIGURE 17. Altitude signal for different sizes of aerostats.

Different sizes of Aerostat envelope generate different buoyancy forces, as shown in Figure 17 above. The Simulink model captures the difference in volume and generates the buoyancy forces accordingly. Greater volume generates a greater buoyancy force that provides more lift.

However, Size 3 Aerostat (0.5 m^2) generates forces that are insufficient to the UAV weight, hence the negative altitude signal.

4.3 Dynamic Stability

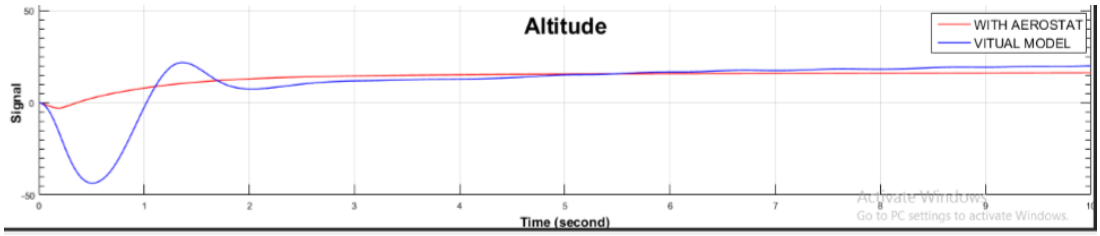

FIGURE 18. Altitude signal for the models with/without an aerostat

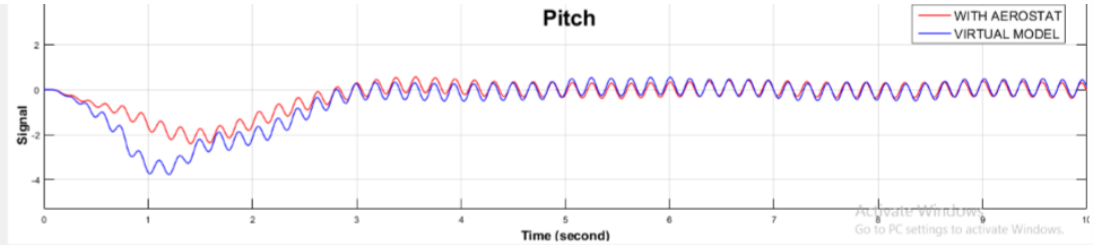

FIGURE 19. Pitch signal for the models with/without an aerostat.

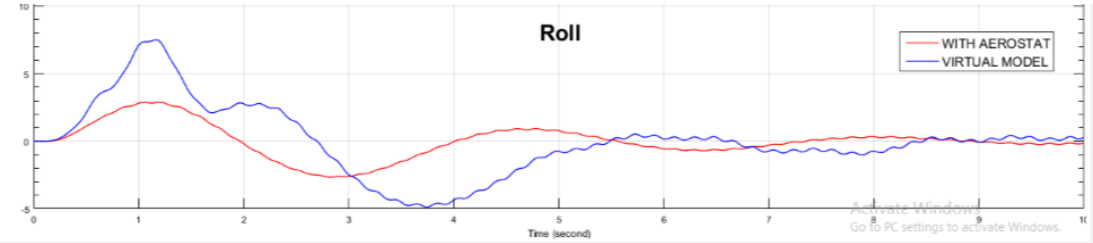

FIGURE 20. Roll signal for the models with/without an aerostat

The dynamic stability for both virtual models; with/without an aerostat were investigated in terms of Altitude, Pitch, and Roll rate.

A difference between signal values are observed in the transient response. The virtual model undergoes negative displacement due to gravity forces (for approximately 0.5 seconds) until the rotors attain speed and generate sufficient lift forces. For the aerostat model, buoyancy forces are exerted directly at t=0.

Moreover, the rotors rotational motion cause dissymmetry in the lift computed by Matlab and cause minor vibrations as a result, unlike the aerostat UAV where the rotors and the vibration effect are cancelled. The discrepancies are further dampened for the aerostat-UAV due to the effect of the added mass, and changes in the overall system inertia.

Moreover, the buoyancy force is exerted at a single point -the center of buoyancy- unlike the four rotors forces exerted at four different points. This reduces the overall system sway.

CHAPTER 5

CONCLUSIONS AND RECOMMENDATIONS

5.1 CONCLUSIONS

The project activities result in a mathematical model of the AR DRONE 2.0 system in Matlab. The software allows for a comprehensive simulation of the flight dynamics and investigation of the dynamic behavior for both the actual UAV and the aerostat equipped system. The model parameters are measured and the results are validated by comparison against real-life model. Furthermore, an aerostat subsystem is added to the model, and buoyancy forces are simulated.

Future works include modification of the system response, by tuning and modifying the controllers' parameters to approximate the real-life behavior of the UAV system, in order to attain an accurate prediction of the combined LTA system behavior.

Conclusively, the project aims to aid further research and development in the field, and facilitate the introduction of improvements and upgrades to the system in order to enhance capabilities and performance.

5.2 RECOMMENDATIONS

In order to improve the accuracy of the analysis, a more detailed mass distribution and physical parameters estimations can be made. This will give flight dynamics with a closer match to the actual UAV.

Moreover, enhancing the aerodynamic design which can be done by either a new aerodynamic analysis or wind tunnel testing with the AR DRONE 2.0. New aerodynamic coefficients will be derived to improve the results of the UAV model.

REFERENCES

[1] A. Rapnett, "Zephyr: A High Altitude Long Endurance Unmanned Air Vehicle," University of Surrey, 2009.

[2] QinetiQ Group PLC, "Zephyr - QinetiQ High-Altitude Long-Endurance (HALE) Unmanned Aerial Vehicle (UAVs)," 2008.

[3] H. Edge, J. Collins, A. Brown , M. Coatney, B. Roget , N. Slegers and A. Johnson, "Lighter-than air and Pressurized structures technology for unmanned aerial vehicles," U.S. Army Resarch Laboratory, Aberdeen proving ground, MD, 2010.

[4] G. A. Khoury, Airship Technology, Cambridge Aerospace, 2012.

[5] T. Luukkonen, "Modelling and control of quadcopter," Aalto University, 2011.

[6] J. Meyer, A. Sendobry, S. Kohlbrecher, U. Klingauf and O. von Stryk, "Comprehensive Simulation of Quadrotor UAVs Using ROS and Gazebo," TU, Darmstadt, Germany, 2012.

[7] A. Tayebi and S. McGilvray, "Attitude stabilization of a four-rotor aerial robot," 43rd IEEE Conference on Decision and Control, Atlantis, 2004.

[8] T. Hamel, M. Robert, R. Lozano and J. Ostrowski, "Dynamic Modelling and COnfiguration Stabilization For an X4-Flyer," in *15th Triennial World Congress*, Barcelona, Spain, 2002.

[9] P. D. A. L. R. Castillo, "Real-time stabilization and tracking of a four rotor mini rotorcraft," *IEEE Trans. Control Syst. Technol.,* vol. 12, no. 4, pp. 510-516, 2004.

[10] P. M. R. H. P. R. J. Pounds, "Design of a four-rotor aerial robot," in *Australian Conf. Robotics and Automation,*, Auckland, Australia, 2002.

[11] P. Pounds, P. Corke and R. Mahony, "Modelling and control of a large quadrotor robot," *Control Engineering Practice,* vol. 18, no. 7, pp. 691-699, 2010.

[12] A. M. G. Rodi´c, "The Mod[eling and Simulation of an Autonomous Quad-," *Acta Polytechnica Hungarica,* vol. 8, no. 4, 2011.

[13] T. Foster, "Dynamic Stability and Handling Qualities of Small Unmanned-Aerial-Vehicles," 2005.

[14] J. Roskam, Airplane Design Part VII: Determination of Stability, Control and Performance Characteristics, 1986.

[15] P. E. Pounds, D. R. Bersak and A. M. Dollar, "Stability of small-scale UAV helicopters and quadrotors with added payload mass under PID control," Springer Science+Business Media, 2011.

[16] M. Samuelsson, "Evaluation of Stability and Flying Qualities of a Light Unmanned Aerial Vehicle (UAV)," 2 August 2012.

[17] D. Grossman, Airships: The Hindenburg and other Zeppelins, 2008.

[18] E. R. Moomey, "Technical Feasibility of Loitering Lighter-Than-Air Near-Space Maneuvering Vehicles.," *Air Force Institute of Technology,* 2005.

[19] C. P. Burgess, "Airship Design," Ronald Auronautic Library, 1927, pp. 289-290.

APPENDIX

FIGURE A.1. Parrot AR DRONE 2.0 original set.

TABLE B.1 Parrot SA AR DRONE 2.0 Specifications. (Source: Parrot SA)

PARTS	SPECIFICATIONS
Camera	• HD Camera. 720p 30fps • Wide angle lens : 92° diagonal • H264 encoding base profile • JPEG photo
Processor	• 1GHz 32 bit ARM Cortex A8 processor with 800MHz video DSP TMS320DMC64x • Linux 2.6.32 • 1Gbit DDR2 RAM at 200MHz
Sensors	• 3 axis gyroscope 2000°/second precision • 3 axis accelerometer +-50mg precision • 3 axis magnetometer 6° precision • Pressure sensor +/- 10 Pa precision • Ultrasound sensors for ground altitude measurement • 60 fps vertical QVGA camera for ground speed measurement
Motors	• 4 brushless inrunner motors. 14.5W 28,500 RMP • Micro ball bearing • Low noise Nylatron gears for 1/8.75 propeller reductor • Tempered steel propeller shaft • Self-lubricating bronze bearing • Specific high propelled drag for great maneuverability • 8 MIPS AVR CPU per motor controller • Fully reprogrammable motor controller • Water resistant motor's electronic controller
Other Hardware	• Carbon fiber tubes : Total weight 380g with outdoor hull, 420g with indoor hull • High grade 30% fibre charged nylon plastic parts • Foam to isolate the inertial center from the engines' vibration • Liquid Repellent Nano-Coating on ultrasound sensors.

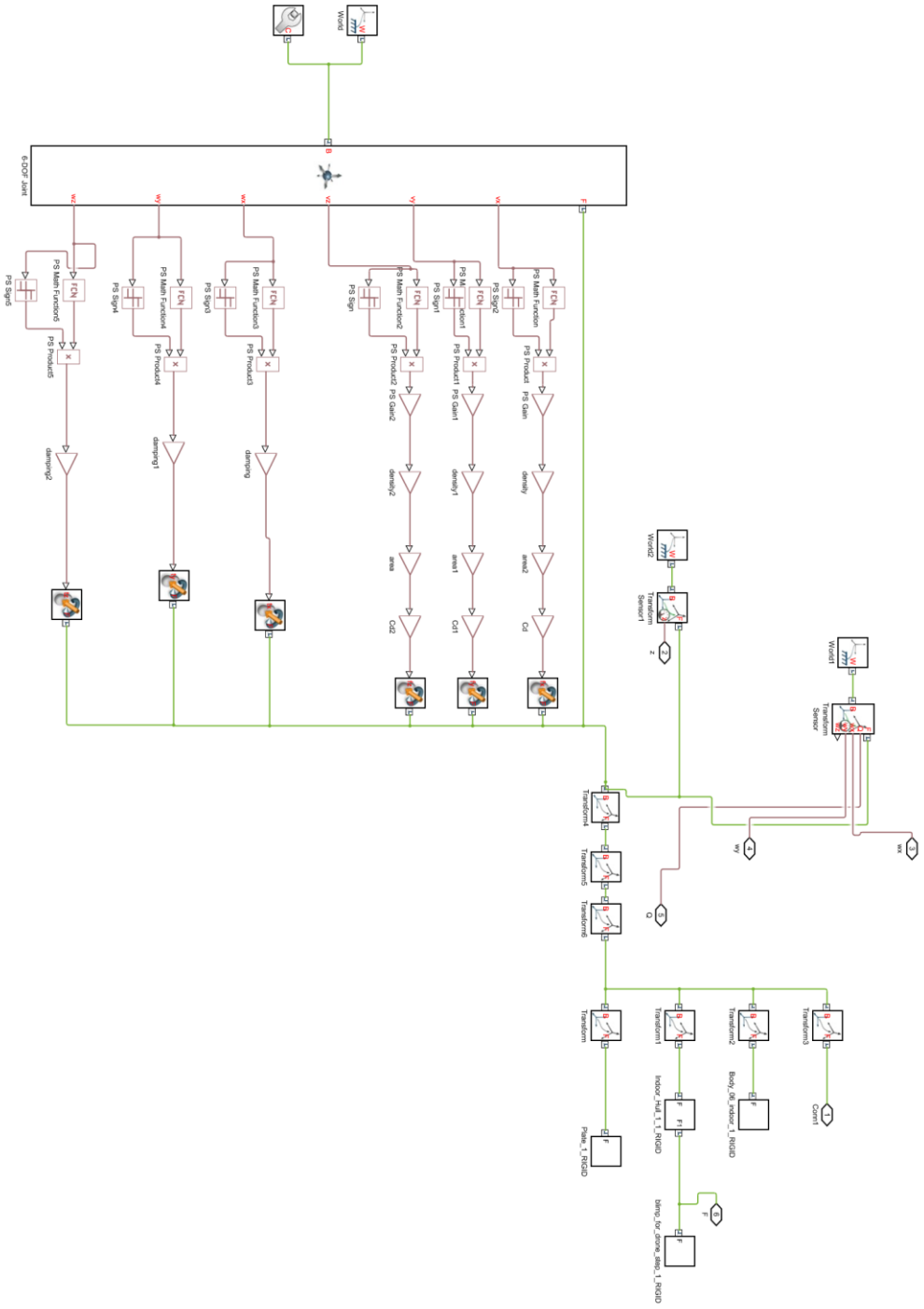

Figure C.1. The complete body dynamics subsystem.